GSA Data Repository Item 2016260

Nanoscale deformation twinning in xenotime, a new shocked mineral, from the Santa Fe impact structure

Aaron J. Cavosie[1,2,3], Pedro E. Montalvo[3], Nicholas E. Timms[1], Steven M. Reddy[1]

[1]TIGeR (The Institute for Geoscience Research), Department of Applied Geology, Curtin University, Perth, WA 6102, Australia

[2]NASA Astrobiology Institute, Department of Geoscience, University of Wisconsin-Madison, Madison WI, 53706, USA

[3]Department of Geology, University of Puerto Rico-Mayagüez, Mayagüez Puerto Rico, 00681 USA

Corresponding author: aaron.cavosie@curtin.edu.au

****

Contents

Item DR1. Field photos and hand sample image of sample 14NM10. **A**: Location of site where sample 14NM10 was collected, in an area of nested shatter cones in granite. **B** and **C**: Photos of shatter cone outcrops within 1-2 meters from the sample collection site. The pen in both images is 13.5 cm long and 1 cm wide. Dashed lines approximate shatter cone surfaces.

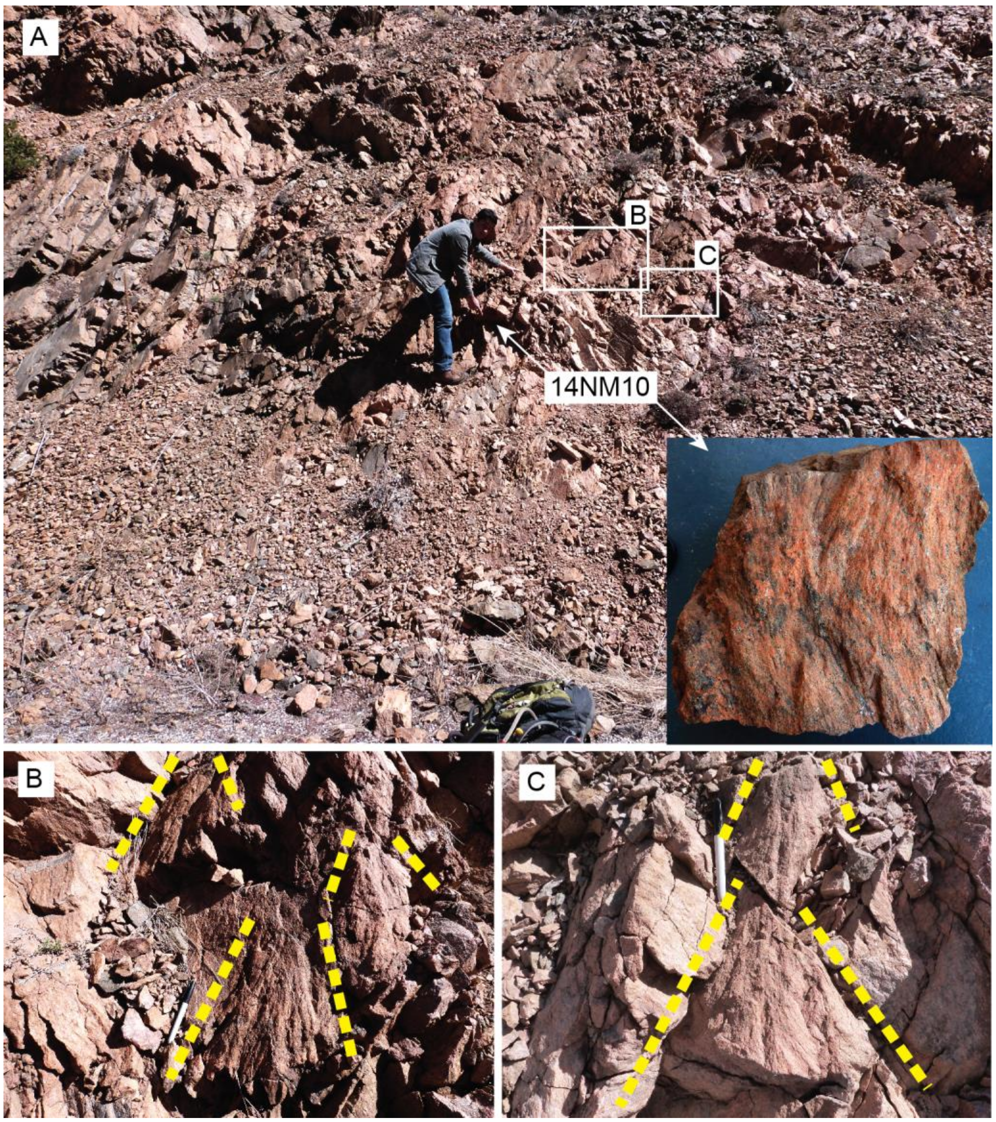

Item DR1 (cont.). Transmitted light images of representative muscovite grains with kink bands in the same thin section of sample 14NM10. Plane polarized light (PPL) images are on the left; cross polarized light (XPL) images are on the right. Each grain contains at least two orientations of kink bands (arrows in PPL image). The dashed line in the XPL images indicates the trace of the basal cleavage. Nearly every grain of muscovite in the thin section has similar kink bands.

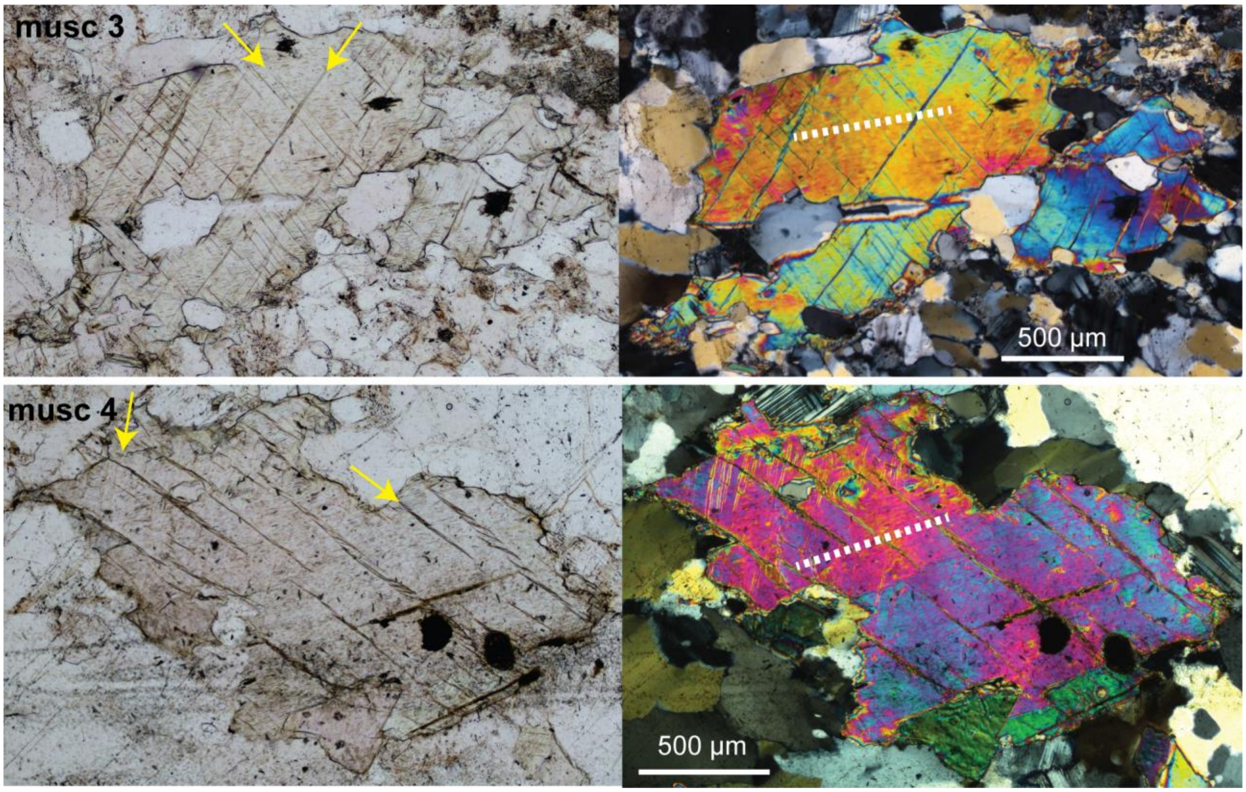

Item DR2. Backscattered electron (BSE) and cathodoluminescence (CL) images of 10 zircon grains in the same thin section of sample 14NM10 that contains the shock-deformed xenotime grains. The image pairs show a BSE image on the left, and a CL image on the right (except for grain 12, bottom row, with only a BSE image). Igneous growth zoning is preserved in many of the grains, as well as dark rims (metamorphic overgrowths?). No definitive shock features were observed in these 10 zircon grains.

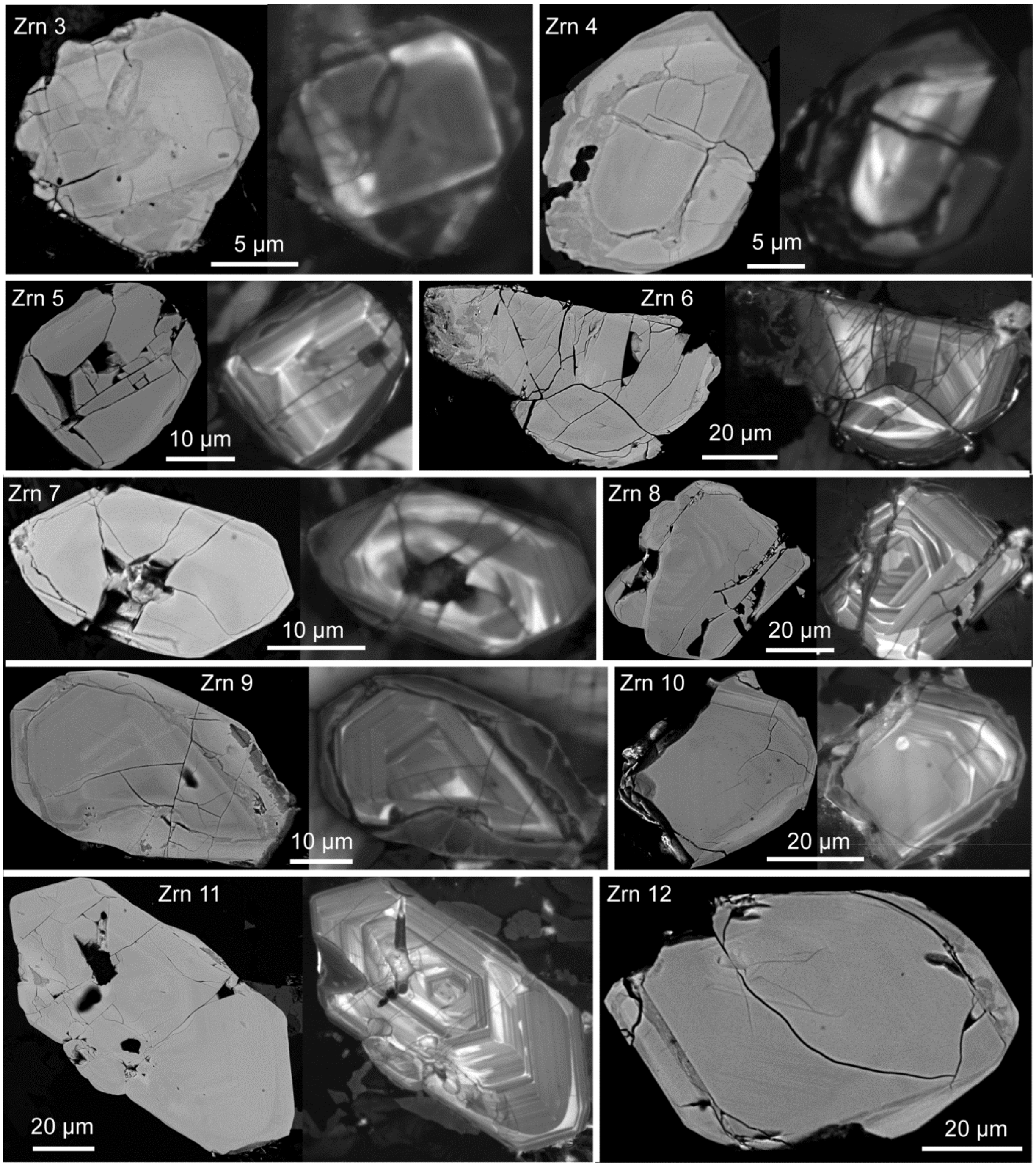

Item DR2 (cont.). Backscattered electron images showing location of the three xenotime grains analyzed relative to the shatter cone surface (SCS). **A.** Xenotime grain 3, near two zircons. Xenotime 3 is located ~ 1.0-1.5 mm from the SCS (not shown, located just beyond edge of image). **B,C.** Xenotime grain 4, located 50 µm from the SCS. **D, E.** Xenotime grain 5, located 400 µm from the SCS. Ks = alkali feldskpar; Mu = muscovite; Qz = quartz.

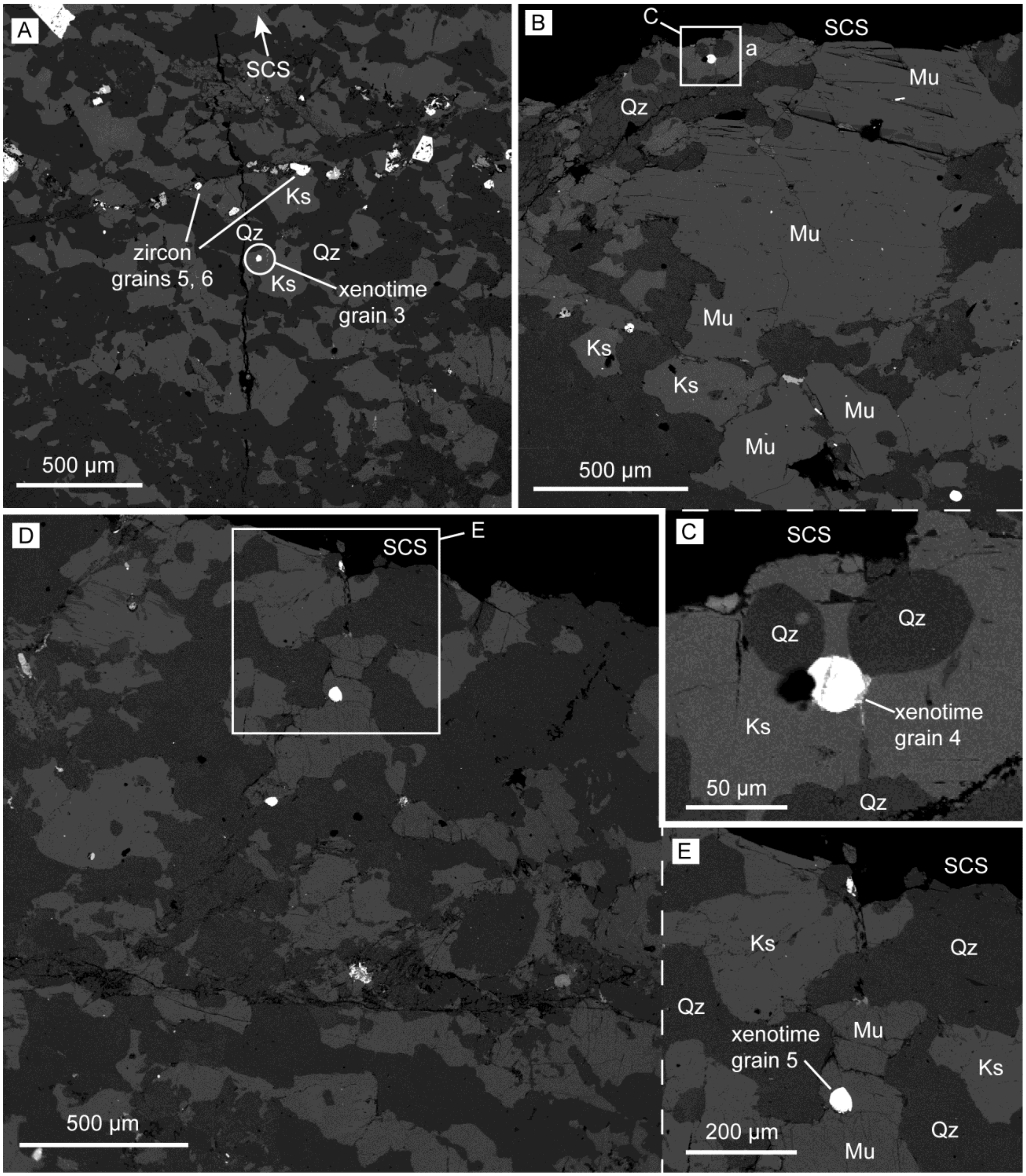

Item DR3. Sample location, preparation and SEM analysis conditions

Sample location

The hand sample 14NM10 was collected in 2014 by P. Montalvo and A. Cavosie. Its location is N35° 43.594’ and W105° 51.449’ (±2.7 m, elevation=2430 m), as measured using the WGS 84 map datum.

Sample preparation

A polished thin section was prepared, and given a final polish with colloidal Si for EBSD analysis.

Scanning electron microscopy

Scanning electron microscopy (SEM) analysis was conducted using a Tescan MIRA3 field emission gun (FEG) SEM at the Microscopy and Microanalysis Facility at Curtin University. The FEG-SEM was used for BSE and panchromatic cathodoluminescence (CL) imaging, and electron backscatter diffraction (EBSD). Automated EBSD maps of regions of interest were generated by indexing electron backscatter diffraction patterns on user-defined grids, and were collected for three xenotime grains. Whole-grain maps were collected using a step size of 50 nm. EBSD analyses were collected with a 20 kV accelerating voltage, 70° sample tilt, 20.5 mm working distance, and 18 nA beam intensity. Electron backscatter patterns were collected with a Nordlys Nano high resolution detector and Oxford Instruments Aztec system using routine data acquisition and noise reduction settings (Table DR1; Reddy et al., 2007). EBSD maps and pole figures were processed using the Tango and Mambo modules in the Oxford Instruments/HKL Channel 5 software package. Full EBSD analysis conditions are listed in Table DR1. Each EBSD map used a match unit for xenotime. Energy dispersive spectroscopy (EDS) elemental maps were collected simultaneously with the EBSD data.

Several types of EBSD images are shown. Band contrast (BC) images (DR item 4) show the relative quality of the electron backscatter diffraction pattern; bright areas can be considered more crystalline, and dark areas less crystalline. Cracks, grain boundaries, radiation damage, and amorphous domains generally are dark to black in BC images. BC images are often combined with other EBSD maps. Texture component (TC) maps show misorientation relative to a reference point, here indicated by a red cross (Fig. 2). Inverse pole figure maps (IPF) show orientation relative to color coded for specific Miller indices (Fig. 3, DR item 4). Pole figures (Fig. 3, DR item 4) are equal area, lower hemisphere stereonet projections. EDS maps show elemental data (DR item 4).

References

Reddy S. M., Timms N. E., Pantleon W., and Trimby T., 2007, Quantitative characterization of plastic deformation of zircon and geological implications: Contributions to Mineralogy and Petrology, v. 153, p. 625–645.

Item DR4. Additional EBSD data for the three xenotime grains. **Grain 3**. **A)** EDS elemental maps of Y, P, O, and Si. **B)** EBSD maps. BC = band contrast; TC = texture component; IPF = inverse pole figure. Red cross in the TC+BC image is the reference point. **C)** Pole figures. Stereo net projections are equal area, lower hemisphere. **D)** Misorientation axis plots. The dominant misorientation relations are low angle boundaries (2-10°) in a broad cluster about <001>.

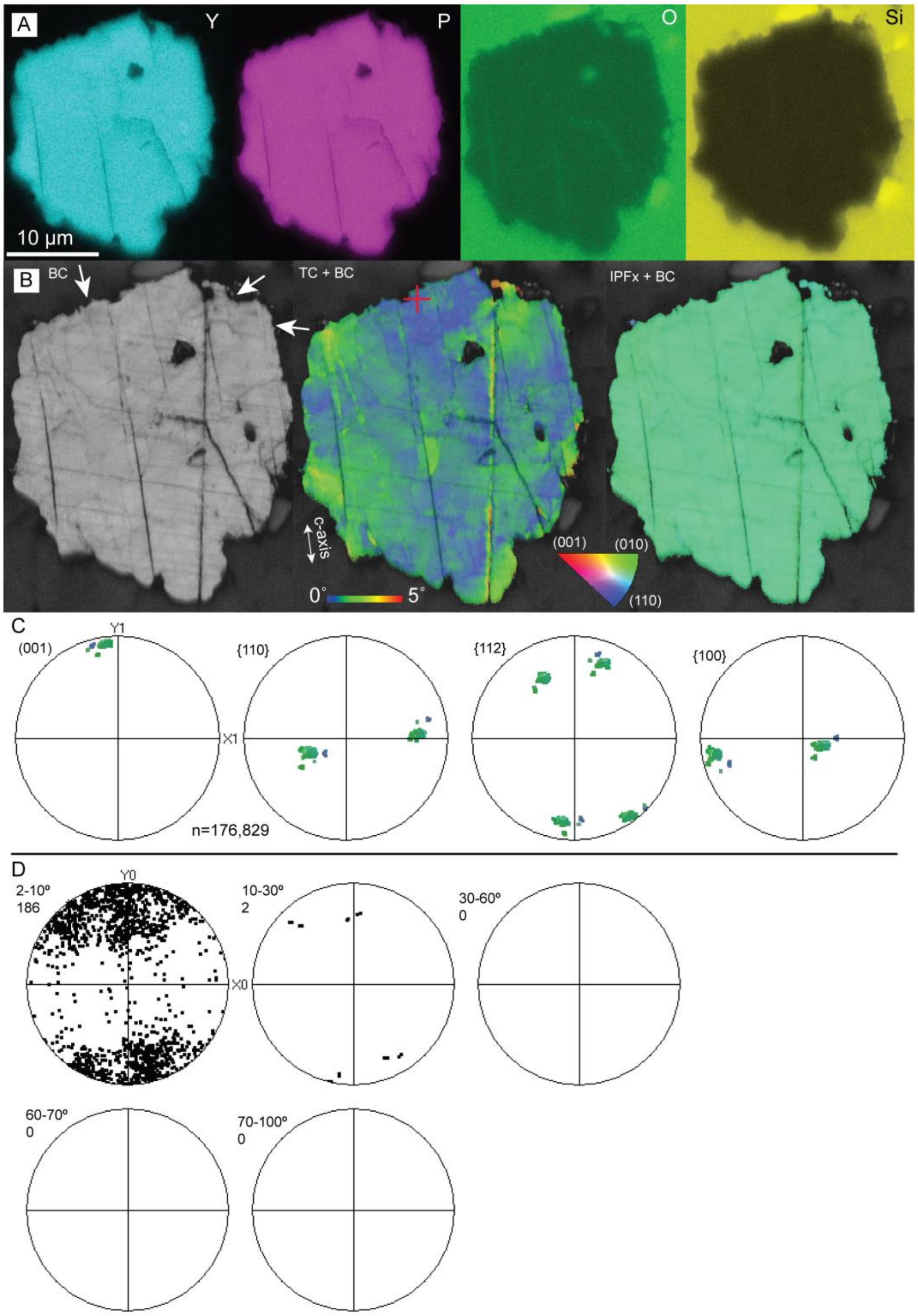

Item DR4 (cont.). Additional EBSD data for the three xenotime grains. **Grain 4**. **A)** EDS elemental maps of Y, P, O, and Si. **B)** EBSD maps. BC = band contrast; TC = texture component; IPF = inverse pole figure. Red cross in TC+BC image is the reference point. **C)** Pole figures. Stereo net projections are equal area, lower hemisphere. **D)** Misorientation axis plots. The dominant misorientation relations are low angle boundaries (2-10°) in a broad cluster about <001> and a small additional cluster about <110>. The high angle (60-70°) misorientation axes about <110> are from the twin lamella.

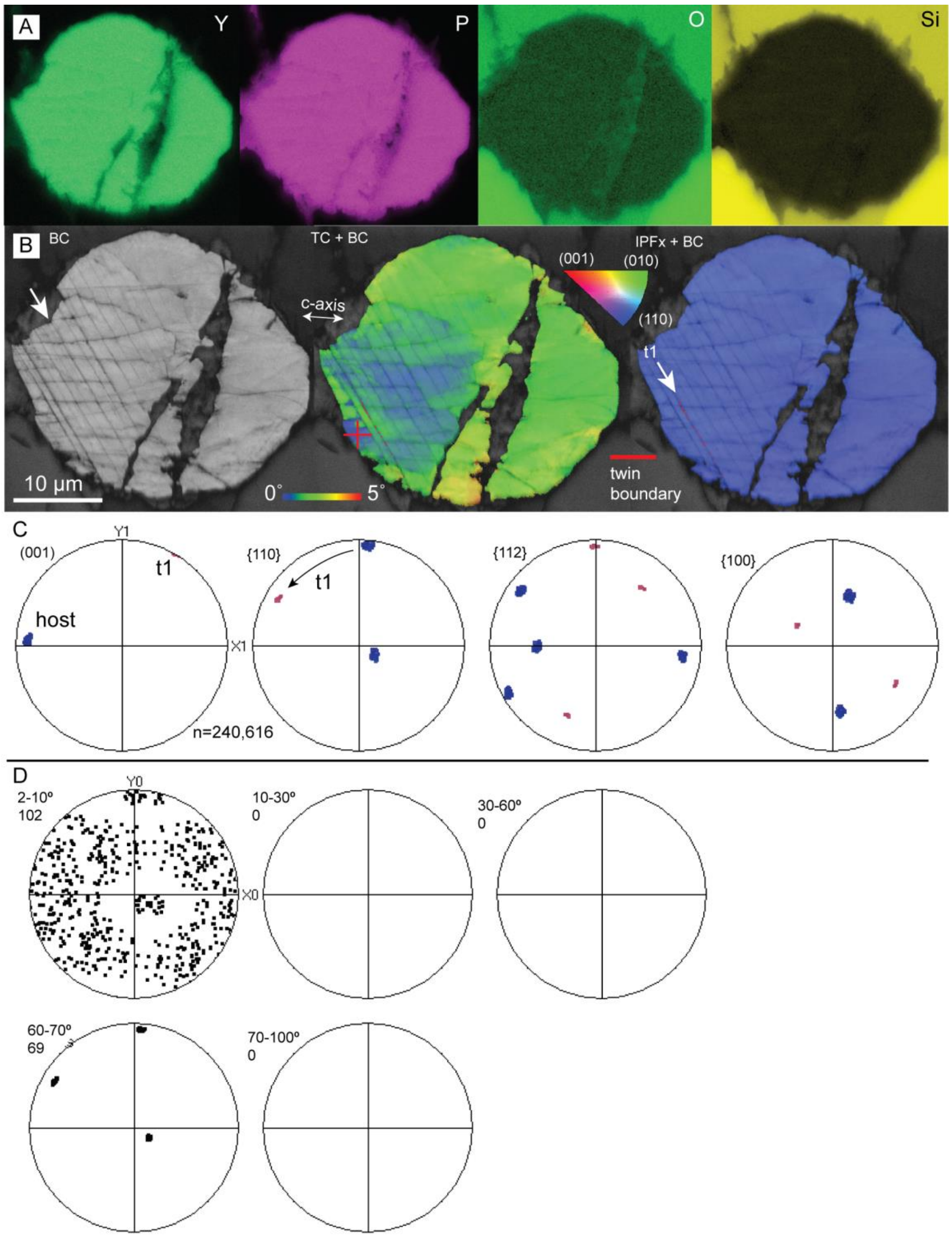

Item DR4 (cont.). Additional EBSD data for the three xenotime grains. **Grain 5**. **A)** EDS elemental maps of Y, P, O, and Si. **B)** EBSD maps. BC = band contrast; TC = texture component; IPF = inverse pole figure. Red cross in TC+BC image is the reference point. **C)** Pole figures. Stereo net projections are equal area, lower hemisphere. **D)** Misorientation axis plots. The dominant misorientation relations are low angle boundaries (2-10°) in a broad cluster about <001>. The high angle (60-70°) misorientation axes about <110> are from the twin lamellae.

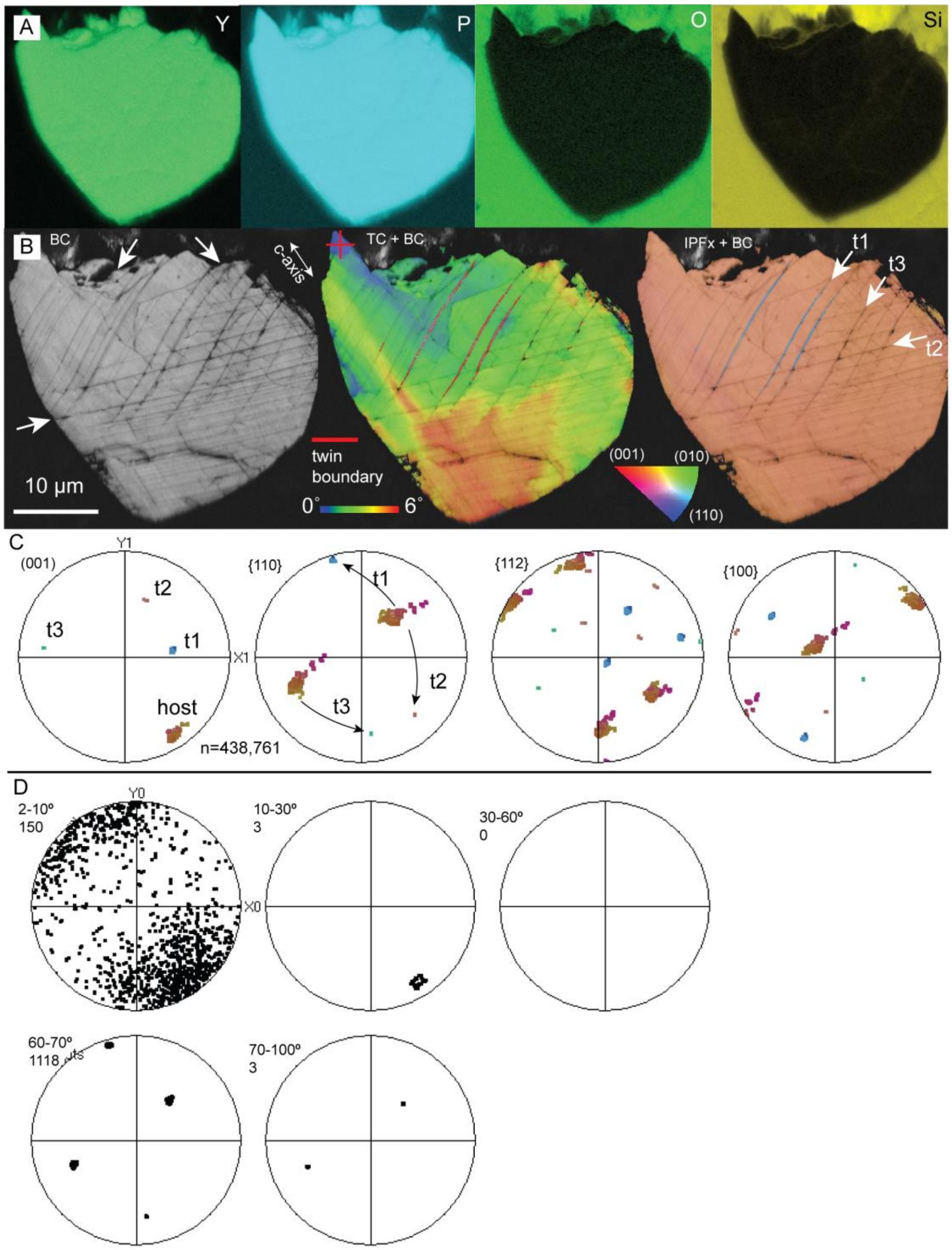

Table DR1. EBSD analysis conditions used for xenotime.

Grain	xeno 3	xeno 4	xeno 5
Shown in figures	2, DR	2, DR	2-3, DR
Thin section 14NM10A			
Acquisition speed (Hz)	40	40	40
Background (frames)	64	64	64
Binning	4 x 4	4 x 4	4 x 4
Gain	High	High	High
Hough resolution	60	60	60
Band detection min/max	6/8	6/8	6/8
Mean angular deviation (xenotime)	0.34	0.32	0.33
X steps	503	682	875
Y steps	618	643	1085
Step distance (nm)	50	50	50
Number of pixels in map	310,854	438,526	949,375
Time for collection (minutes)	118	181	391
Noise reduction methods			
Wildspike	yes	yes	yes
n neighbour zero solution extrapolation	no	no	no
Kuwahara Filter	no	no	no
SEM Model: Tescan Mira3 FEG-SEM			
EBSD system: Nordlys Detector- Aztec			
Match unit: Xenotime(Y), from the Inorganic Crystal Structure Database. Structural data from Milligan et al. (1982).			
Grains were in a thin section, mounted flat, and grounded with Cu tape. The sample was rotated to a 70° tilt by moving the stage. The sample was coated with a thin (<5 nm) carbon coat. The accelerating voltage was 20 kV. The working distance was 20.5 mm.			
xeno = xenotime. DR = Data Repository			